International Journal of Radiation Biology

ISSN: 0955-3002 (Print) 1362-3095 (Online) Journal homepage: http://www.tandfonline.com/loi/irab20

Differential response of normal and transformed mammary epithelial cells to combined treatment of anti-miR-21 and radiation

Vanja Radulovic, Theresa Heider, Sabine Richter, Simone Moertl, Michael J. Atkinson & Nataša Anastasov

To cite this article: Vanja Radulovic, Theresa Heider, Sabine Richter, Simone Moertl, Michael J. Atkinson & Nataša Anastasov (2017): Differential response of normal and transformed mammary epithelial cells to combined treatment of anti-miR-21 and radiation, International Journal of Radiation Biology, DOI: 10.1080/09553002.2016.1266057

To link to this article: http://dx.doi.org/10.1080/09553002.2016.1266057

INTERNATIONAL JOURNAL OF RADIATION BIOLOGY, 2017
http://dx.doi.org/10.1080/09553002.2016.1266057

Taylor & Francis
Taylor & Francis Group

ORIGINAL ARTICLE

OPEN ACCESS

Differential response of normal and transformed mammary epithelial cells to combined treatment of anti-miR-21 and radiation

Vanja Radulovic[a], Theresa Heider[a], Sabine Richter[a], Simone Moertl[a], Michael J. Atkinson[a,b] and Nataša Anastasov[a]

[a]Institute of Radiation Biology, Helmholtz Center Munich, German Research Center for Environmental Health, Neuherberg, Germany; [b]Chair of Radiation Biology, Technical University of Munich, Munich, Germany

ABSTRACT

Purpose: MicroRNA miR-21 has emerged as a therapeutic target in the treatment of breast cancer. This study was designed to compare the responses of breast cancer cells and non-transformed breast epithelial cells to a combined regimen of miR-21 inhibition and radiation.

Materials and methods: The MDA-MB-361 (breast cancer) and MCF-10A (non-transformed mammary epithelial) cell lines were used for the comparison in this in vitro study. The stable knockdown of miR-21 was performed by using lentiviral approach. The response of the cells was monitored 4, 24 and 48 h after the irradiation with 0.25 and 2.5 Gy, using sham-irradiated cells as controls. The response of the cells was established by performing various functional assays – cell viability and cell attachment, clonogenic survival, cell cycle analysis and 3D microtissue formation.

Results: The knockdown of miR-21 induced significant increase in apoptosis and growth delay in MDA-MB-361 cancer cells compared to non-transformed MCF-10A cells. After combined radiation and anti-miR-21 treatment, MDA-MB-361 cells show reduced cell growth and viability what is presented in their inability to form colonies. MCF-10A cells were not as sensitive to the combined treatment and that has also been confirmed with colony forming assay.

Conclusions: Cellular response to a combined treatment of anti-miR-21 and radiation is different between cancer and non-cancer cells which highly support the idea of linking miR-21 inhibitor and radiation treatment in the future therapeutic approaches for breast cancer.

ARTICLE HISTORY
Received 21 July 2016
Revised 20 October 2016
Accepted 4 November 2016

KEYWORDS
Cellular response; MCF-10A; miR-21; radiation oncology

Introduction

miRNAs are a class of short, non-coding, single-stranded post-transcriptional regulators of gene expression (Bartel 2004). Since miRNAs can regulate translation of a broad set of mRNAs they hold a great potential for cancer therapy (Liu et al. 2014; Price & Chen 2014). It has become evident that dysregulation of miRNAs is an emerging hallmark of cancer, in the tumor itself as well as in its surrounding microenvironment (McManus 2003; Lu et al. 2005).

Both anti-miRNAs and mimics of miRNAs have been developed as therapeutic strategies with several miRNA modulators having entered clinical trials (Croce 2009; Kasinski & Slack 2011; Liu et al. 2014). With the goal of improving cancer treatment responses, this kind of therapy can be used alone (Cheng et al. 2013; Poltronieri et al. 2013; Sicard et al. 2013) or in combination with currently existing ones such as radiotherapy (Liu et al. 2014).

MicroRNA-21 (miR-21) is overexpressed in several human cancers including breast cancer, glioblastoma (Yang et al. 2014) and pancreatic cancer (Sicard et al. 2013). The higher expression of miR-21 is significantly associated with adverse clinicopathological factors and a worse prognosis, suggesting it may act as a cellular oncomiR (Medina et al. 2010; Anastasov et al. 2012). miR-21 targets multiple pathways including the genes related to cell cycle regulation. Previous studies have shown that miR-21 affects cellular proliferation and migration in human breast cancer cells (Yan et al. 2011). Moreover, as miR-21 can promote radioresistance (Anastasov et al. 2012; Gwak et al. 2012; Summerer et al. 2015), inhibitors of miR-21 may present an effective approach for modifying radiosensitivity (Zhang & Ma 2012; Liu et al. 2014). For the maximum benefit however, a targeted anti-miR-21 therapy should not increase the sensitivity of normal mammary epithelial cells to radiation.

We have therefore compared the responses of the breast cancer (MDA-MB-361) and non-transformed epithelial (MCF-10A) cells to the treatment with a miR-21 inhibitor (anti-miR-21) and radiation. MCF-10A are non-tumorigenic breast epithelial cells, obtained from a patient with benign fibrocystic disease with a spontaneous mutation (deletion in the

CONTACT Nataša Anastasov natasa.anastasov@helmholtz-muenchen.de Institute of Radiation Biology, Helmholtz Center Munich-German Research Center for Environmental Health, Ingolstädter Landstraße 1, 85764 Neuherberg, Germany

Supplemental data for this article can be accessed here.

p16/ARF locus) that contributes to their immortalization (Soule et al. 1990). These cells are frequently used for the comparative study of the effects of treatments on normal versus malignant mammary epithelial cells (Glaysher et al. 2014).

Materials and methods

Cell lines and culture conditions

MCF-10A cells were cultured in DMEM/F12 supplemented with 5% horse serum, 0.5 mg/ml hydrocortisone, 20 ng/ml EGF, 10 μg/ml insulin and 100 ng/ml cholera toxin. MDA-MB-361 and HEK293T cells were cultured in high Glucose DMEM culture medium supplemented with 20% or 10% fetal bovine serum, respectively. All cell lines were cultivated at 37 °C and 5% CO_2. Cells were seeded in six-well plates at 200,000 cells per well for subsequent analysis, unless otherwise stated. Cell counting was performed using Z™ Series Coulter Counter® (Beckman Coulter, CA, USA). All cells were authenticated by genetic profiling (Eurofins MWG Operon, Ebersberg, Germany) with STR matching analysis (DSMZ, Heidelberg, Germany), and tested as mycoplasma free with MycoAlert™ Mycoplasma Detection Kit (Lonza, Cologne, Germany).

Irradiation

Irradiation was performed using a Cs-137 source (HWM D-2000, Wälischmiller Engineering, Germany) at a dose rate of 0.5 Gy/min. Doses of 0.25 and 2.5 Gy were administered at room temperature and control cells were sham irradiated. Each treatment was performed with three technical replicates and repeated at least three times (biological replicates; $n = 3$).

Lentivirus production

The lentiviral transduction vector pGreenPuro (pGP; System Biosciences, Mountain View, CA, USA) was used as the backbone for cloning the miR-21 knockdown sequence (anti-miR-21) using the miRNA oligo (pmiRZIP-21; Cat. No. MZIP21-PA-1-GVO-SB; Biocat, Heidelberg, Germany) and lentivirus production was performed as previously described in HEK293T cells (Anastasov et al. 2009; Hofig et al. 2012). Empty pGP vector was used as control for lentivirus production (further in paper labelled as EV – empty vector).

Transduction of breast epithelial cell lines

Transduction of MCF-10A and MDA-MB-361 cells with either anti-miR-21 or control lentivirus (EV) was performed using protocols previously described (Anastasov et al. 2010; Hofig et al. 2012). Briefly, 2×10^5 cells per well were infected with 3×10^5 lentiviral transduction units (TU) (multiplicity of infection [MOI] = 1.5) with the addition of synperonic (100 μg/ml) and polybrene (10 μg/ml) as adjuvants. After 24 h of incubation (at 37 °C and 5% CO_2), the medium was changed and cells were incubated for an additional 48 h in adequate medium with the inclusion of puromycin (0.3 μg/ml) before further analysis.

RNA isolation for miRNA expression analysis

Total RNA was isolated 4 and 24 h after irradiation. Cells were trypsinized and pelleted by centrifugation at 2000 rpm for 5 min, and washed twice with 1 ml of PBS. Total RNA was isolated from the cells using the mirVana™ miRNA isolation kit (Applied Biosystems; Foster City, CA, USA) according to the manufacturer's instructions. The concentration of total RNA was determined with the Nanodrop spectrophotometer (PeqLab Biotechnology, Germany).

TaqMan-miRNA assays and data analysis

A TaqMan-miRNA assay (Cat. No. 4427975; Assay ID 000397, Applied Biosystems, Forster City, CA, USA) was used for miR-21-5p expression analysis. The qRT-PCR was performed using a StepOnePlus Detection System (Applied Biosystems, Foster City, CA). The relative expression values of specific miRNA were calculated by using the $2^{-\Delta\Delta CT}$ method (Anastasov et al. 2012) normalized to a RNU44 (Cat. No. 4427975; Assay ID 001095) as endogenous control and to the sham-irradiated control of each cell line.

Cell viability and cell attachment assays

The number of viable cells in culture was determined using CellTiter-Glo® Luminescent Cell Viability Assay (Promega, Madison, WI, USA) according to the manufacturer's instructions; 24 h before irradiation, 1000–5000 cells were seeded per well into opaque-walled 96-well plates (Corning, NY, USA). The assay was performed 24 and 48 h after irradiation. Luminescence was recorded using a spectrophotometer plate reader (Tecan, Switzerland). Cell detachment was monitored by counting the number of cells in the supernatant 24 and 48 h after irradiation. The number of attached cells was measured 48 h after irradiation by trypsinizing, collecting and counting the cells using Z™ Series Coulter Counter® (Beckman Coulter, CA, USA).

Clonogenic survival

For the measurement of clonogenic survival, cells were seeded in six-well plates at a range of densities (500–12,000 cells per well) and 24 h later sham treated or irradiated with 2, 4, 6 and 8 Gy. After 7–21 days (depending on the cell line), the colony formation capacity was assessed after fixation with 100% ethanol and subsequent staining with Giemsa solution (diluted 1:10 in PBS). The colonies with more than 30 cells were counted.

Cell cycle analysis

Cell cycle distribution was analysed 24 h after irradiation as previously described (Nusse et al. 1994; Anastasov et al. 2012). Treated cells were trypsinized and the pellets were

collected by centrifugation at 300 *g* for 5 min after which the supernatant was carefully removed. The cell pellet was resuspended in 500 µl of solution I (10 mM NaCl, 4 mM Na-citrate, 10 µg/ml RNase, 0.3% Nonidet P-40, and 50 µg/ml propidiumiodide [PI]) and incubated in the dark at room temperature for 60 min which was followed by addition of 500 µl of solution II (70 mM citric acid, 250 mM sucrose and 50 µg/ml PI). Cell cycle distribution analyses were performed using a FACScan LSR II (excitation wavelength: 488 nm; emission wavelength: 610 nm) and a BD FACSDiva™ software (BD Biosciences, Heidelberg, Germany). Cells with a DNA content lower than that of cells in the G1 phase of the cell cycle (<2n) were defined as the subG1 fraction and were considered to be apoptotic.

3D microtissue analyses

The breast epithelial cells were seeded with 2000 cells per drop into scaffold-free 96-well InSphero culture GravityPLUS™ plates (InSphero AG, Schlieren, Switzerland). 3D microtissues were produced within 3 days and transferred into InSphero GravityTRAP™ plates. After 24 h (defined as day 0 of treatment), microtissues were sham irradiated (0 Gy) or irradiated with a single dose of 0.25 or 2.5 Gy. Growth of eight spheroids per treatment was monitored every 3 days using a high content screening system Operetta (Perkin Elmer, Waltham, MA) and quantified in maximal area of GFP expressing microtissue (μm^2) using the Harmony analysis Software (Perkin Elmer) (Anastasov et al. 2015; Falkenberg et al. 2016).

Statistical analysis

Biological replicates were analysed by Student's *t*-test. Statistical significance was defined as *p*-value less than 0.05 as follows: $^{*}p < 0.05$, $^{**}p < 0.01$, $^{***}p < 0.001$. Data presented as mean ± SEM.

Results

miR-21 expression in MCF-10A and MDA-MB-361 cells after exposure to radiation

Previous studies have established that miR-21 is overexpressed in breast cancer cells compared to the normal breast tissues (Sempere et al. 2007; Si et al. 2007). The level of miR-21 in the MDA-MB-361 mammary cancer cell line was 3.99 ± 0.01-fold higher than that of MCF-10A non-transformed mammary epithelial cells (Figure 1(a)).

miR-21 levels were significantly upregulated in MCF-10A cells after 0.25 Gy (1.65 ± 0.02-fold) and 2.5 Gy dose of radiation (1.63 ± 0.06-fold), 24 h after exposure (Figure 1(b)). In

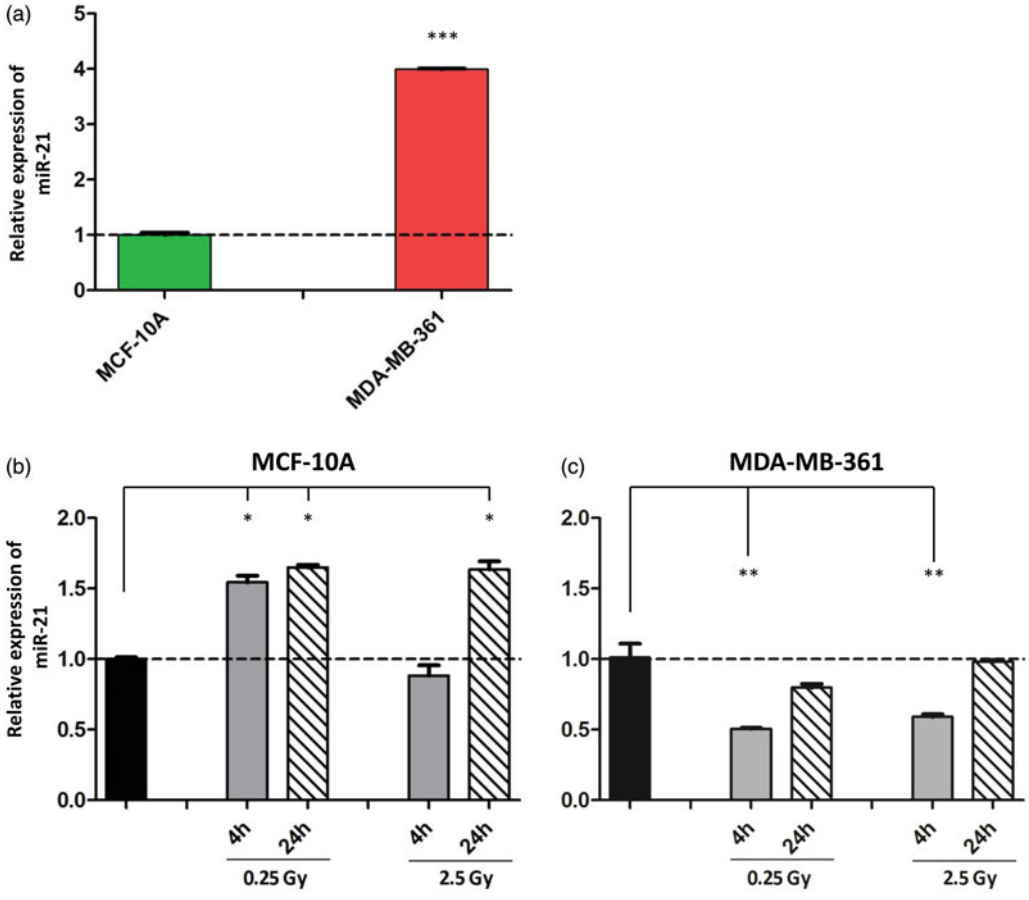

Figure 1. miR-21 expression in MCF-10A and MDA-MB-361 cells after exposure to radiation. (a) Relative expression of endogenous miR-21 presented as fold change after normalization to RNU44 and to non-transformed mammary epithelial cells MCF-10A (set as 1). Relative miR-21 expression in MCF-10A (b) and MDA-MB-361 (c) cells 4 and 24 h after exposure to 0.25 and 2.5 Gy doses of irradiation, in correlation to the expression of sham-irradiated controls at each time-point. Data represent means ± SEM ($n = 3$). Student's *t*-test was used for statistical analysis. $^{*}p < 0.05$, $^{**}p < 0.01$, $^{***}p < 0.001$.

contrast, miR-21 expression was downregulated in MDA-MB-361 after 0.25 Gy (0.50 ± 0.01-fold) and 2.5 Gy (0.59 ± 0.02-fold) 4 h or not significantly changed 24 h post-irradiation (Figure 1(c)).

Cellular response to miR-21 inhibition and radiation

The knockdown of miR-21 was done using the lentiviral transduction of the cells. The effectiveness of lentiviral transduction was determined using cytofluorimetric analysis (FACS) to detect GFP expression in the cells. MCF-10A cells show 86.34% and 92.76% transduction efficiency with EV and anti-miR-21, respectively (Figure 2(a)), whereas MDA-MB-361 cells show 98.40% (EV) and 99.37% (anti-miR-21) GFP positive expressing cells (Figure 2(b)). The level of miR-21 expression was analysed 72 h after transduction and in both cell lines miR-21 expression is decreased to 0.38 ± 0.04 (MCF-10A) and 0.34 ± 0.01 (MDA-MB-361) compared to the levels of miR-21 in control (EV) cells that was set to 1 (Figure 2(c,d)).

The cellular response to combined miR-21 inhibition and radiation was studied by exposing control cells and lentiviraly transduced cells to 0.25 and 2.5 Gy dose of radiation. After 24 h, differences between the cell lines were apparent with combined irradiation and anti-miR-21 treatment (Figure 3).

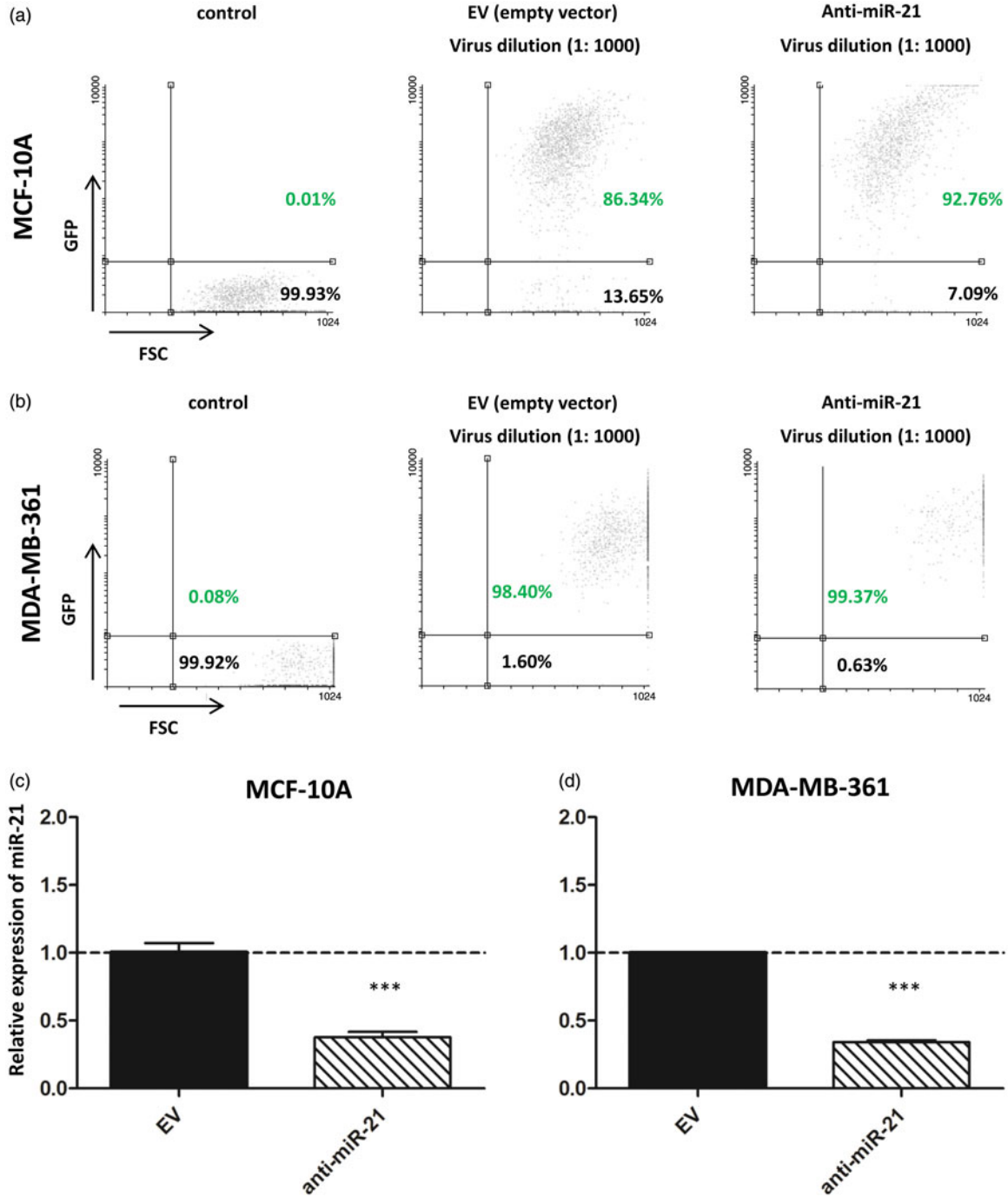

Figure 2. miR-21 knockdown in MCF-10A and MDA-MB-361 cells. GFP detection using cytofluorometric analysis (FACS) of MCF-10A (a) and MDA-MB-361 cells (b) transduced with empty lentivirus (EV) or miR-21 knockdown (anti-mir-21) virus. Percentage of cells expressing GFP after lentiviral infection is shown. miR-21 expression levels 72 h after lentiviral transduction with anti-miR-21 in MCF-10A (c) and MDA-MB-361 cells (d). Data represent means ± SEM ($n = 3$). $^{***}p < 0.001$.

The potent influence of anti-miR-21 and 2.5 Gy irradiation on tumor cells (MDA-MB-361) was detected (Figure 3(b)).

Knockdown of miR-21 without radiation reduces the cell viability from 2.26 ± 0.08 (EV at 0 Gy) to 1.29 ± 0.09 for anti-mir-21 at 0 Gy (Figure 4(a)) in MCF-10A and correspondingly from 0.84 ± 0.01 (EV) to 0.46 ± 0.02 (anti-miR-21) in MDA-MB-361 cells (Figure 4(b)). Treatment with radiation (both 0.25 and 2.5 Gy) does not significantly change the viable cell fraction after 24 h. Cell viability after 48 h shows increase in MCF-10A viable cell fraction after combined anti-miR-21 and radiation treatment (1.69 ± 0.02 after 2.5 Gy) indicating their ability to further proliferate after the treatment. Unlike MCF-10A, MDA-MB-361 cells show slight decrease (0.37 ± 0.01 after 2.5 Gy) in proliferation capacity 48 h after combined

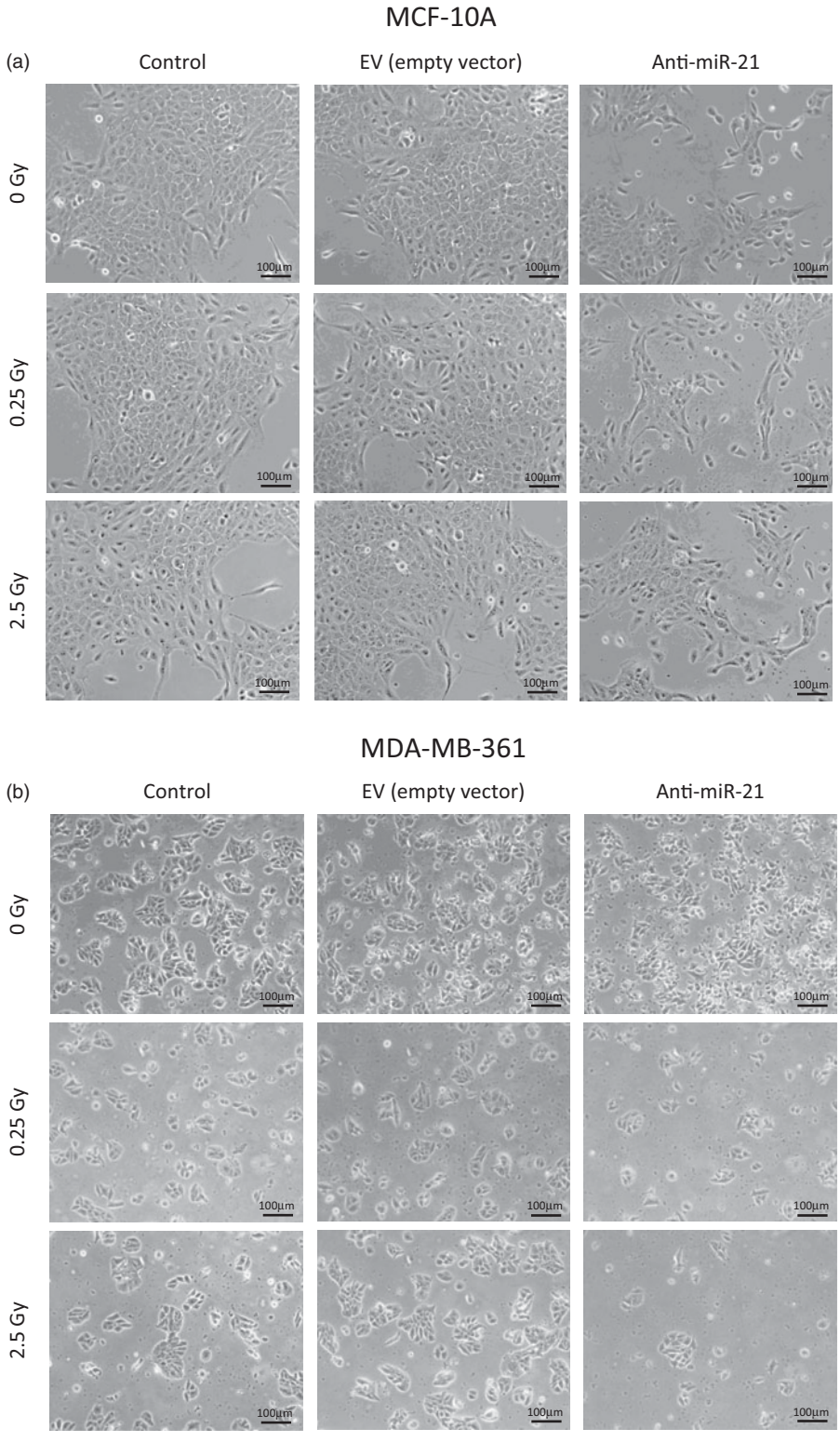

Figure 3. Morphology of MCF-10A (a) and MDA-MB-361 (b) control cells (without lentiviral transduction) and cells transduced with EV and anti-miR-21, 24 h after 0.25 and 2.5 Gy irradiation. Scale bar =100 μm.

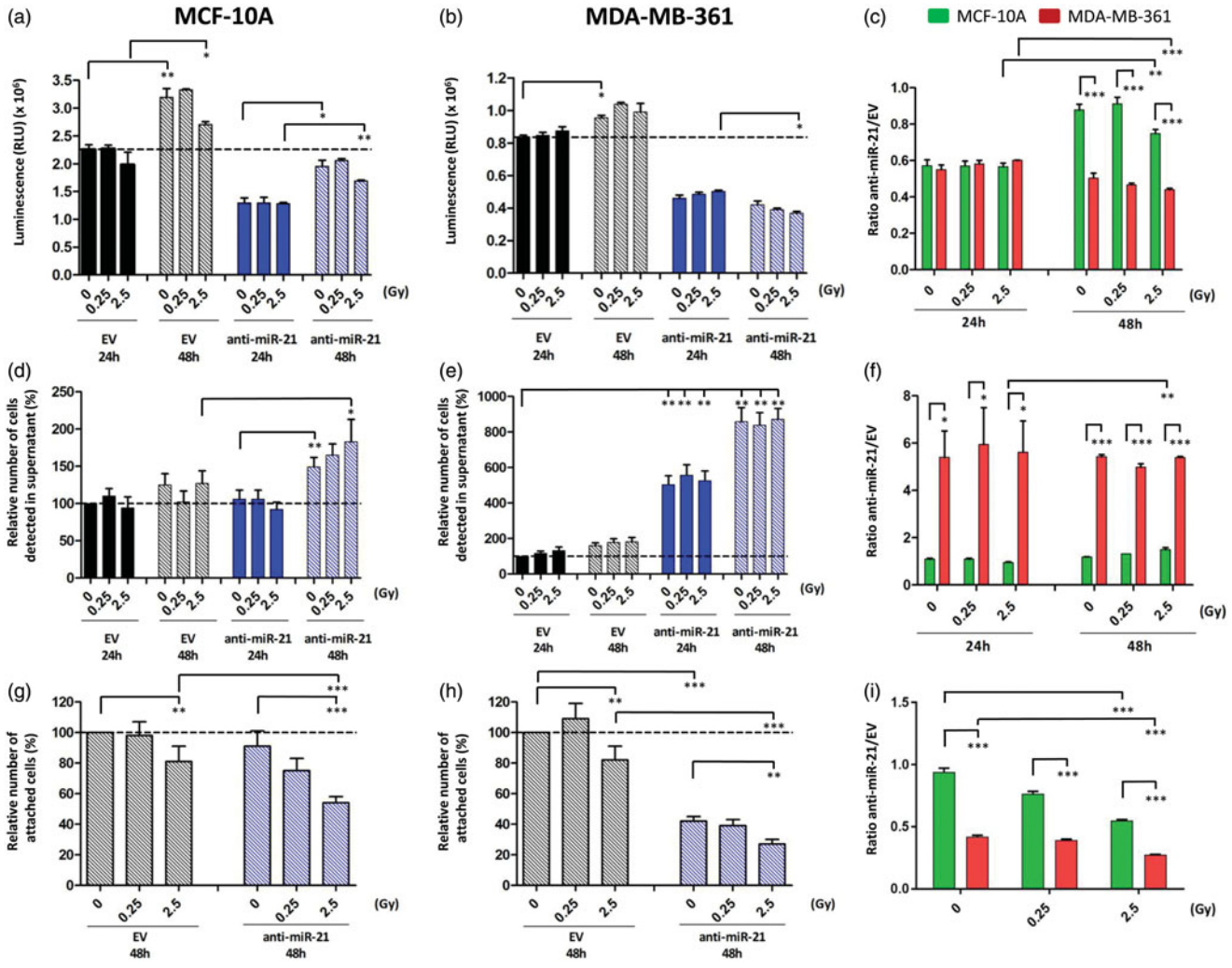

Figure 4. MDA-MB-361 cells show lower viability and attachment ability after miR-21 knockdown compared to MCF-10A cells. Viability of MCF-10A (a) and MDA-MB-361 cells (b) was determined 24 and 48 h after irradiation and their values are presented as relative luminescent units (RLU) corrected with blank medium controls. Dash line represents the luminescent signal of sham-irradiated EV control at 24-h time-point. The ratio of anti-miR-21 to EV luminescent signal (anti-miR-21/EV) after 0.25 and 2.5 Gy radiation doses is shown on part (c). Relative cell attachment ability was measured by monitoring the number of cells in supernatant (d, e) 24 and 48 h and by quantifying the number of attached cells (g, h) 48 h after irradiation. The anti-miR-21/EV ratio of cells detected in supernatant (f) and attached cells (i) are shown. Normalization was performed to the value of sham-irradiated EV cells (24 h – d, e; 48 h – g, h) that has been set to 100%. Data represent means ± SEM ($n = 3$). Student's t-test was used for statistical analysis. $^{*}p < 0.05$, $^{**}p < 0.01$, $^{***}p < 0.001$.

treatment. Low dose irradiation (0.25 Gy) in both cell lines does not show significant differences to sham-irradiated cells. No significant differences in cell viability between control cells (non-virally transduced) and EV (empty vector transduced) cells were detected (Supplementary Figure S1, available online).

The luminescent signal ratio of anti-miR-21 and EV cells shows that 24 h after radiation cell viability is similar between two cell lines while at 48 h more viable MCF-10A cells are detected compared to MDA-MB-361 cells (Figure 4(c)).

The number of detached MCF-10A cells (Figure 4(d)) slightly increases after miR-21 knockdown 48 h post-irradiation (0 Gy – 149 ± 13% versus 2.5 Gy – 183 ± 30% compared to 24-h EV time-point analysis). MDA-MB-361 (Figure 4(e)) shows significant increase after miR-21 knockdown and irradiation 24 and 48 h after treatment (504 ± 51% after 24 h and 858 ± 79% after 48 h post irradiation, compared to EV control of 24-h time-point). Radiation has not significantly changed the cell detachment (compared to sham-irradiated cells) in both cell lines used for analysis. The ratio of detached anti-miR-21 and EV cells is higher for MDA-MB-361 cell line compared to MCF-10A (Figure 4(f)).

In parallel, the number of attached cells quantified 48 h after miR-21 knockdown demonstrates the significant decrease of the MDA-MB-361 cell ability to attach (42 ± 5%) (Figure 4(h)) that is not the case with MCF-10A (91 ± 10%) (Figure 4(g)). The dose of 2.5 Gy combined with anti-miR-21 additionally decrease the number of attached cells and the effect was more visible for MDA-MB-361 (27 ± 3%) than for MCF-10A (54 ± 5%) cells. In MCF-10A (Figure 4(g)) and MDA-MB-361 (Figure 4(h)) low dose irradiation (0.25 Gy) does not have any additional effect compared to sham-irradiated cells. The ratio of attached anti-miR-21 and EV cells shows that MDA-MB-361 cells, after miR-21 knockdown, attach less than MCF-10A (Figure 4(i)) that correlates with results above (Figure 4(f)).

Further, we have noticed the differences between MCF-10A and MDA-MB-361 in ability to form colonies after miR-21 knockdown. There is no significant difference in colony formation between MCF-10A treated with anti-miR-21 and

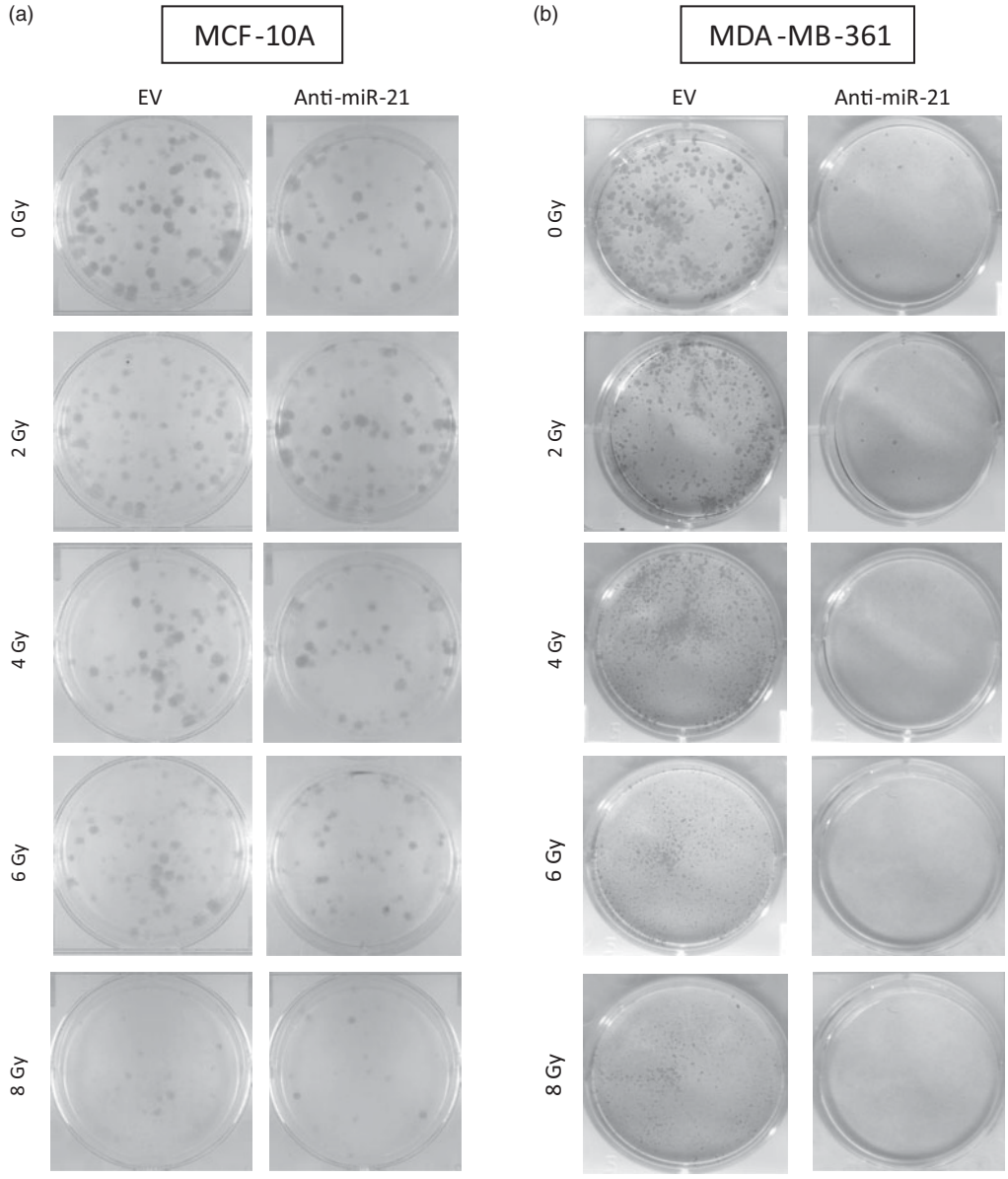

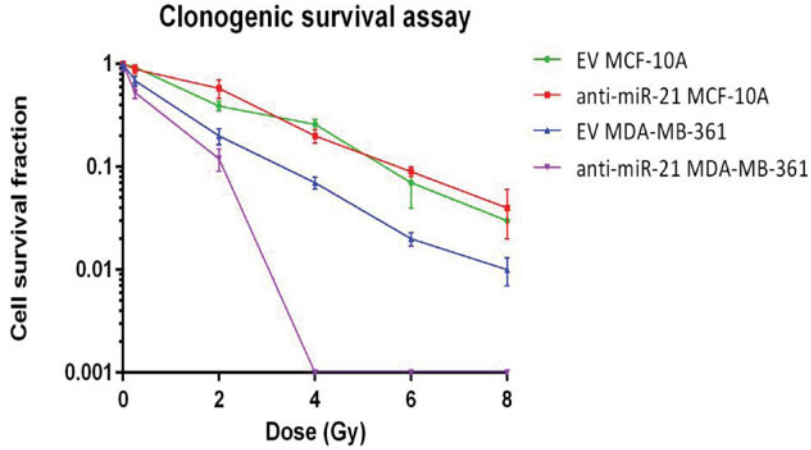

Figure 5. miR-21 knockdown influences clonogenic ability of MDA-MB-361 cells. Pictures of clonogenic survival assay for MCF-10A (a) and MDA-MB-361 (b) cells after different doses of irradiation. Clonogenic survival assay data (c) represent means ± SEM ($n = 4$).

EV (control cells) 7 days after irradiation (Figure 5(a)). MDA-MB-361 cells with anti-miR-21 are not able to form colonies even without radiation (Figure 5(b)). These data are in agreement with results above, confirming the low capability of MDA-MB-361 cells to attach (Figure 4(h)).

miR-21 downregulation increases subG1 and reduces the G2 cell fraction in MDA-MB-361 but not in MCF-10A cells

After downregulation of miR-21 we could detect differences in cell cycle distributions between MCF-10A (Figure 6(a)) and MDA-MB-361 (Figure 6(b)). miR-21 knockdown does not significantly change the population of MCF-10A cells (Figure 6(c)) in subG1 phase compared to the control (EV) while the MDA-MB-361 subG1 cell population number (Figure 6(d)) is significantly increased after anti-miR-21 not only after 2.5 Gy irradiation (3.59 ± 0.07) but also in sham (3.45 ± 0.39) and 0.25 Gy (3.83 ± 0.19) irradiated cells. The significant increase in MDA-MB-361 subG1 fraction compared to MCF-10A cells is confirmed by anti-miR-21 and EV treated cells ratio (Figure 6(e)).

The anti-miR-21 slightly reduces the number of MCF-10A cells in G2 phase (Figure 6(f)) with no significant reduction when combined with radiation. MDA-MB-361 cells (Figure 6(g)) show prominent reduction in number of cells in G2 phase after miR-21 knockdown. Significant decrease in MDA-MB-361 G2 phase compared to MCF-10A is confirmed by anti-miR-21 and EV-treated cells ratio, after 2.5 Gy irradiation (Figure 6(h)). No significant differences in cell cycle analysis were detected between control cells and EV treated cells in both MCF-10A and MDA-MB-361 cell line (Supplementary Figure S2).

Anti-miR-21 and radiation effects using 3D-microtissue growth analysis

Both MCF-10A and MDA-MB-361 cells were able to form 3D-microtissues. MCF-10A cells treated with anti-miR-21 do not show growth delay compared to EV control (Figure 7(a)). A growth delay of MDA-MB-361 with anti-miR-21 was observed (compared to EV) with an additional growth delay after 2.5 Gy irradiation (Figure 7(b)). Combined anti-miR-21 and radiation treatment effect is evident for the tumor cells (MDA-MB-361) using 3D microtissue analysis what is in correlation with results obtained in 2D cell culture, where the difference in cellular response to combined treatment between MCF-10A and MDA-MB-361 cells was identified. The quantified 3D microtissue (region area in μm^2) and corresponding ratio of anti-miR-21 and EV (Figure 7(c)) indicates that the growth ability of MDA-MB-361, after miR-21 knockdown, is decreased when compared to MCF-10A and to sham irradiated MDA-MB-361 microtissues.

Discussion

We have investigated the influence of combined lentiviral miR-21 knockdown and radiation treatment using breast cancer (MDA-MB-361) and non-tumorigenic breast epithelial cells (MCF-10A). The levels of endogenous miR-21 expression are higher in MDA-MB-361 cells compared to MCF-10A. This is consistent with high levels of miR-21 reported in breast tumors in comparison to normal surrounding epithelial cells (Krichevsky & Gabriely 2009). Previous work has shown that miR-21 is upregulated in different human cells in culture after irradiation (Shi et al. 2012; Cellini et al. 2014) that is confirmed with observed increase in miR-21 expression (24 h) after irradiation using MCF-10A cells. In contrast, not significant changes were detected in the MDA-MB-361 cancer cells, 24 h after exposure to radiation. Differential miR-21 response to radiation could be potentially dependent on (4-fold) higher endogenous miR-21 expression levels in cancer cells compared to non-tumorigenic breast epithelial cells. Presented data indicate the miR-21 significance as specific cancer therapy target for the future.

It has been shown that miR-21 overexpression may promote radioresistance (Anastasov et al. 2012) and even reduce responsiveness to cytotoxic targeted therapies (Gong et al. 2011) in breast cancers. Thus, the use of miR-21 inhibitors is a strategy that may increase the sensitivity of cancer cells to radiation (Anastasov et al. 2012; Ma et al. 2014), but its potential impact on surrounding non cancer cells is still unexplored.

Breast conserving surgery followed by external beam radiation therapy represents the standard of care for the majority of breast cancer patients (Early Breast Cancer Trialists' Collaborative 2011). Whilst adjuvant radiotherapy can improve the locoregional control and overall survival (Ragaz et al. 2005) it may induce moderate-to-intense skin reaction in 85–95% of patients, and less frequently second cancer development (Hill et al. 2001). It is estimated that less than 10% of phase I cancer clinical trials combine chemical and radiation therapy analysis (Glaysher et al. 2014) and it is of great importance to elucidate potential side-effects of new targeted therapies applying comprehensive preclinical analysis. Thus, there is a need for a novel treatment strategy or agent to protect normal tissues from radiation therapy damage, without compromising or enhancing the killing effect of radiation on tumors which includes development of radiosensitizers (Tinoco et al. 2013).

Previous studies have shown that G2/M cell cycle arrest upon irradiation can predict the level of radioresistance of tumor cells (Liu et al. 2014). Herewith, we present that anti-miR-21 treatment is able to reduce G2 phase in MDA-MB-361 more than in MCF-10A cells (Figure 6(f,g)). The observed reduction of G2 could potentially explain reduced cell viability and increased number of detached tumor cells (MDA-MB-361, Figure 4(e)). Such specific effects on tumor cells are in agreement with results of changes in G2 block that were reported previously for breast cancer, colon cancer and glioblastoma cell lines (Wang et al. 2009; Yan et al. 2011; Anastasov et al. 2012). miRNAs that upregulated in cancers are termed oncomiRs (Esquela-Kerscher & Slack 2006) and miR-21 as one of the first described (Folini et al. 2010) has a crucial role in tumor cell proliferation (Meng et al. 2007), apoptosis (Chan et al. 2005), invasion and metastasis (Asangani et al. 2008). Possible explanation why MCF-10A cells react differently

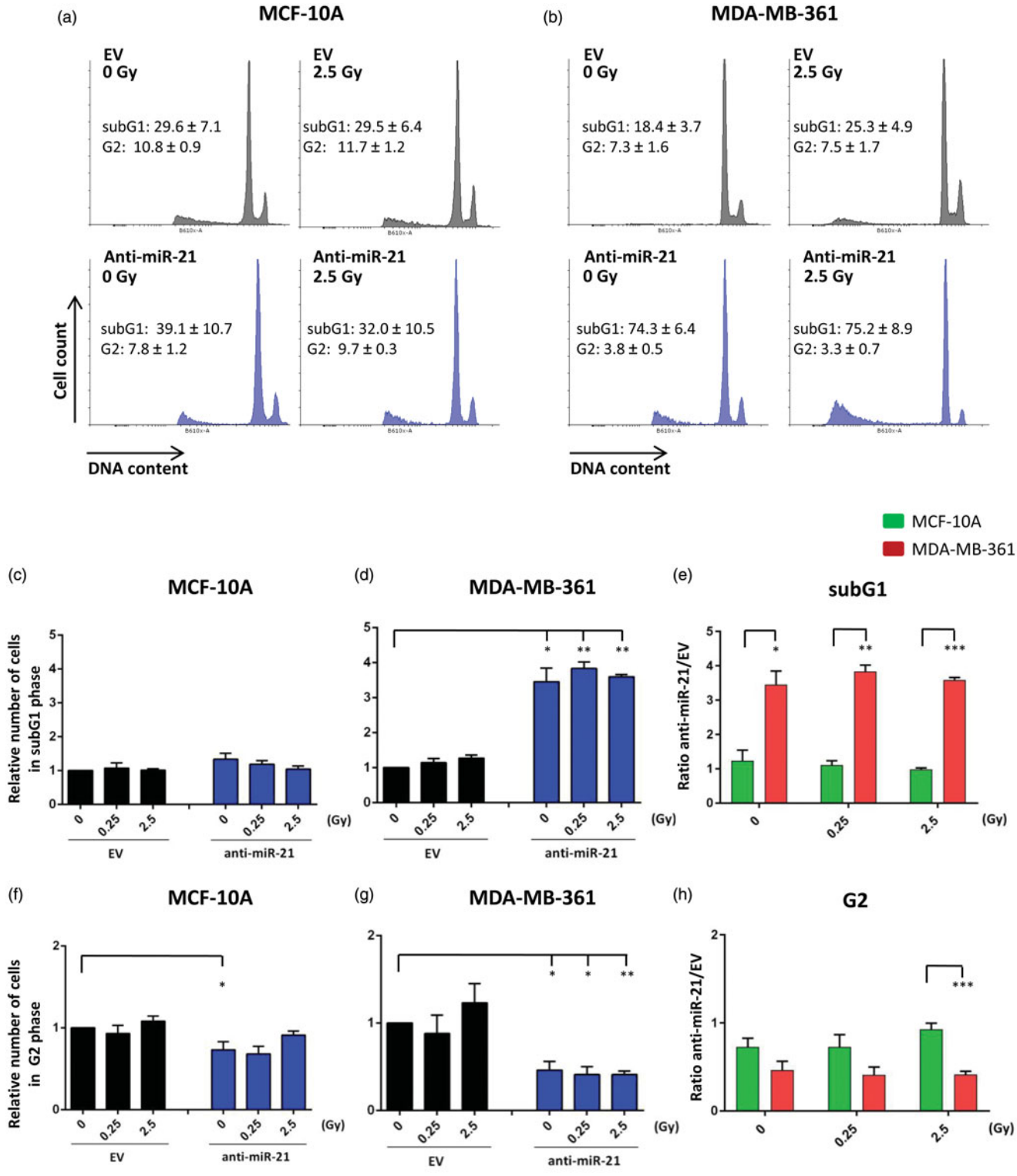

Figure 6. miR-21 downregulation significantly increases subG1 fraction and affects G2 phase in MDA-MB-361. Representative FACS analysis of sham irradiated and cells exposed to 2.5 Gy irradiation of MCF-10A (a) and MDA-MB-361 (b). Both cell lines were infected with empty lentivirus (EV) or miR-21 knockdown (anti-miR-21) and analysed for cell cycle changes 24 h after 0.25 and 2.5 Gy irradiation. Relative number of cells in subG1 (c,d) and G2 (f,g) phases of cell cycle presented as fold change after normalization to sham irradiated EV cells. The anti-miR-21/EV ratio of cells detected in subG1 (e) and G2 (h) phase of cell cycle are presented. Data represent means ± SEM ($n = 3$). Student's t-test was used for statistical analysis. $^{*}p < 0.05$, $^{**}p < 0.01$.

to combined treatment with anti-miR-21 and radiation than breast cancer cells, could be 'oncomiR addiction' (Sharma & Settleman 2007; Medina et al. 2010). The cancer cells can depend on oncomiR expression and its downregulation can have potent effect on their survival. Therefore, at the moment miR-21 presents a good candidate and further supports the idea of using miR-21 inhibitors in order to treat human cancers (Sicard et al. 2013; Najafi et al. 2015).

In conclusion, we show that miR-21 knockdown induces apoptosis and growth arrest in breast cancer cells (MDA-MB-361) but not in breast non-tumorigenic epithelial cells (MCF-10A). These findings confirm the potential use of

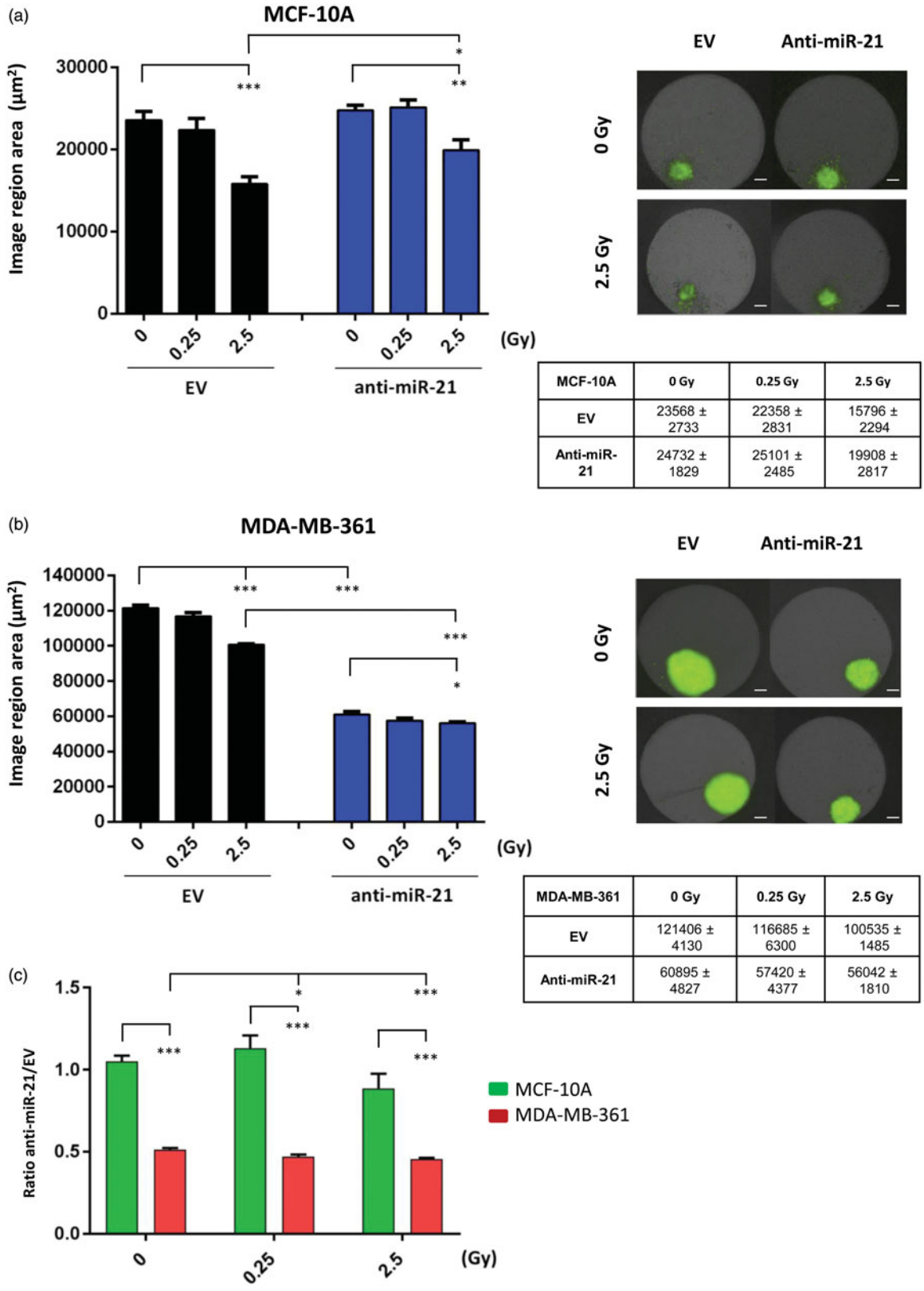

MCF-10A	0 Gy	0.25 Gy	2.5 Gy
EV	23568 ± 2733	22358 ± 2831	15796 ± 2294
Anti-miR-21	24732 ± 1829	25101 ± 2485	19908 ± 2817

MDA-MB-361	0 Gy	0.25 Gy	2.5 Gy
EV	121406 ± 4130	116685 ± 6300	100535 ± 1485
Anti-miR-21	60895 ± 4827	57420 ± 4377	56042 ± 1810

Figure 7. Growth analysis of 3D-microtissues of MCF-10A and MDA-MB-361 cells with constitutive lentiviral GFP expression. 3D-microtissue growth analysis after radiation-quantification of spheroid growth delay after 0.25 and 2.5 Gy (9 days after radiation treatment) of MCF-10A (a) and MDA-MB-361 (b). The ratio of anti-miR-21 and EV for each dose of radiation is presented at part (c). Tables present the original values of image region area (µm^2) detected. Data represent means ± SEM ($n = 3$). Representations of Operetta GFP quantification (EV and anti-miR-21) after indicated time points (9th day after seeding in assay plates after 0 and 2.5 Gy doses of radiation). Student's t-test was used for statistical analysis. *$p < 0.05$, **$p < 0.01$, ***$p < 0.001$. Scale bar =100 µm.

miR-21 as a main target for the development of new breast cancer therapeutical strategies. Our results show that miR-21 inhibition exclusively in breast cancer cells could hold a significant therapeutic value for breast cancer patients and further investigations in this field are necessary.

Acknowledgements

The authors thank Rosemarie Kell for excellent technical assistance and Janine König for using her pictures of MDA-MB-361 cells. This work was supported by the EURATOM Fission, European Commission 7th Framework Programme, Dark.Risk project (contract number 323216).

Disclosure statement

The authors report no conflicts of interest. The authors alone are responsible for the content and writing of the paper.

References

Anastasov N, Bonzheim I, Rudelius M, Klier M, Dau T, Angermeier D, Duyster J, Pittaluga S, Fend F, Raffeld M, et al. 2010. C/EBPbeta expression in ALK-positive anaplastic large cell lymphomas is required for cell proliferation and is induced by the STAT3 signaling pathway. Haematologica. 95:760–767.

Anastasov N, Hofig I, Radulovic V, Strobel S, Salomon M, Lichtenberg J, Rothenaigner I, Hadian K, Kelm JM, Thirion C, et al. 2015. A 3D-microtissue-based phenotypic screening of radiation resistant tumor cells with synchronized chemotherapeutic treatment. BMC Cancer. 15:466.

Anastasov N, Höfig I, Vasconcellos IG, Rappl K, Braselmann H, Ludyga N, Auer G, Aubele M, Atkinson MJ. 2012. Radiation resistance due to high expression of miR-21 and G2/M checkpoint arrest in breast cancer cells. Radiat Oncol. 7:206.

Anastasov N, Klier M, Koch I, Angermeier D, Höfler H, Fend F, Quintanilla-Martinez L. 2009. Efficient shRNA delivery into B and T lymphoma cells using lentiviral vector-mediated transfer. J Hematopathol. 2:9–19.

Asangani IA, Rasheed SA, Nikolova DA, Leupold JH, Colburn NH, Post S, Allgayer H. 2008. MicroRNA-21 (miR-21) post-transcriptionally downregulates tumor suppressor Pdcd4 and stimulates invasion, intravasation and metastasis in colorectal cancer. Oncogene. 27:2128–2136.

Bartel DP. 2004. MicroRNAs: genomics, biogenesis, mechanism, and function. Cell. 116:281–297.

Cellini F, Morganti AG, Genovesi D, Silvestris N, Valentini V. 2014. Role of microRNA in response to ionizing radiations: evidences and potential impact on clinical practice for radiotherapy. Molecules (Basel, Switzerland). 19:5379–5401.

Chan JA, Krichevsky AM, Kosik KS. 2005. MicroRNA-21 is an antiapoptotic factor in human glioblastoma cells. Cancer Res. 65:6029–6033.

Cheng CJ, Saltzman WM, Slack FJ. 2013. Canonical and non-canonical barriers facing AntimiR cancer therapeutics. CMC. 20:3582–3593.

Croce CM. 2009. Causes and consequences of microRNA dysregulation in cancer. Nat Rev Genet. 10:704–714.

Early Breast Cancer Trialists' Collaborative G. 2011. Effect of radiotherapy after breast-conserving surgery on 10-year recurrence and 15-year breast cancer death: meta-analysis of individual patient data for 10,801 women in 17 randomised trials. Lancet. 378:1707–1716.

Esquela-Kerscher A, Slack FJ. 2006. Oncomirs: microRNAs with a role in cancer. Nat Rev Cancer. 6:259–269.

Falkenberg N, Hofig I, Rosemann M, Szumielewski J, Richter S, Schorpp K, Hadian K, Aubele M, Atkinson MJ, Anastasov N. 2016. Three-dimensional microtissues essentially contribute to preclinical validations of therapeutic targets in breast cancer. Cancer Med. 5:703–710.

Folini M, Gandellini P, Longoni N, Profumo V, Callari M, Pennati M, Colecchia M, Supino R, Veneroni S, Salvioni R, et al. 2010. miR-21: an oncomir on strike in prostate cancer. Mol Cancer. 9:12.

Glaysher S, Bolton LM, Johnson P, Torrance C, Cree IA. 2014. Activity of EGFR, mTOR and PI3K inhibitors in an isogenic breast cell line model. BMC Res Notes. 7:397.

Gong C, Yao Y, Wang Y, Liu B, Wu W, Chen J, Su F, Yao H, Song E. 2011. Up-regulation of miR-21 mediates resistance to trastuzumab therapy for breast cancer. J Biol Chem. 286:19127–19137.

Gwak HS, Kim TH, Jo GH, Kim YJ, Kwak HJ, Kim JH, Yin J, Yoo H, Lee SH, Park JB. 2012. Silencing of microRNA-21 confers radio-sensitivity through inhibition of the PI3K/AKT pathway and enhancing autophagy in malignant glioma cell lines. PLoS One. 7:e47449.

Hill RP, Rodemann HP, Hendry JH, Roberts SA, Anscher MS. 2001. Normal tissue radiobiology: from the laboratory to the clinic. Int J Radiat Oncol Biol Phys. 49:353–365.

Hofig I, Atkinson MJ, Mall S, Krackhardt AM, Thirion C, Anastasov N. 2012. Poloxamer synperonic F108 improves cellular transduction with lentiviral vectors. J Gene Med. 14:549–560.

Kasinski AL, Slack FJ. 2011. Epigenetics and genetics. MicroRNAs en route to the clinic: progress in validating and targeting microRNAs for cancer therapy. Nat Rev Cancer. 11:849–864.

Krichevsky AM, Gabriely G. 2009. miR-21: a small multi-faceted RNA. J Cell Mol Med. 13:39–53.

Liu J, Zhu H, Yang X, Ge Y, Zhang C, Qin Q, Lu J, Zhan L, Cheng H, Sun X. 2014. MicroRNA-21 is a novel promising target in cancer radiation therapy. Tumor Biol. 35:3975–3979.

Lu J, Getz G, Miska EA, Alvarez-Saavedra E, Lamb J, Peck D, Sweet-Cordero A, Ebert BL, Mak RH, Ferrando AA, et al. 2005. MicroRNA expression profiles classify human cancers. Nature. 435:824–838.

Ma Y, Xia H, Liu Y, Li M. 2014. Silencing miR-21 sensitizes non-small cell lung cancer A549 cells to ionizing radiation through inhibition of PI3K/Akt. BioMed Res Int. 2014:617868.

McManus MT. 2003. MicroRNAs and cancer. Semin Cancer Biol. 13:253–258.

Medina PP, Nolde M, Slack FJ. 2010. OncomiR addiction in an *in vivo* model of microRNA-21-induced pre-B-cell lymphoma. Nature. 467:86–90.

Meng F, Henson R, Wehbe-Janek H, Ghoshal K, Jacob ST, Patel T. 2007. MicroRNA-21 regulates expression of the PTEN tumor suppressor gene in human hepatocellular cancer. Gastroenterology. 133:647–658.

Najafi Z, Sharifi M, Javadi G. 2015. Degradation of miR-21 induces apoptosis and inhibits cell proliferation in human hepatocellular carcinoma. Cancer Gene Ther. 22:530–535.

Nusse M, Beisker W, Kramer J, Miller BM, Schreiber GA, Viaggi S, Weller EM, Wessels JM. 1994. Measurement of micronuclei by flow cytometry. Methods Cell Biol. 42 Pt B:149–158.

Poltronieri P, D'Urso PI, Mezzolla V, D'Urso OF. 2013. Potential of anticancer therapy based on anti-miR-155 oligonucleotides in glioma and brain tumours. Chem Biol Drug Des. 81:79–84.

Price C, Chen J. 2014. MicroRNAs in cancer biology and therapy: current status and perspectives. Genes Dis. 1:53–63.

Ragaz J, Olivotto IA, Spinelli JJ, Phillips N, Jackson SM, Wilson KS, Knowling MA, Coppin CM, Weir L, Gelmon K, et al. 2005. Locoregional radiation therapy in patients with high-risk breast cancer receiving adjuvant chemotherapy: 20-year results of the British Columbia randomized trial. J Natl Cancer Inst. 97:116–126.

Sempere LF, Christensen M, Silahtaroglu A, Bak M, Heath CV, Schwartz G, Wells W, Kauppinen S, Cole CN. 2007. Altered MicroRNA expression confined to specific epithelial cell subpopulations in breast cancer. Cancer Res. 67:11612–11620.

Sharma SV, Settleman J. 2007. Oncogene addiction: setting the stage for molecularly targeted cancer therapy. Genes Develop. 21:3214–3231.

Shi Y, Zhang X, Tang X, Wang P, Wang H, Wang Y. 2012. MiR-21 is continually elevated long-term in the brain after exposure to ionizing radiation. Radiat Res. 177:124–128.

Si ML, Zhu S, Wu H, Lu Z, Wu F, Mo YY. 2007. miR-21-mediated tumor growth. Oncogene. 26:2799–2803.

Sicard F, Gayral M, Lulka H, Buscail L, Cordelier P. 2013. Targeting miR-21 for the therapy of pancreatic cancer. Mol Ther. 21:986–994.

Soule HD, Maloney TM, Wolman SR, Peterson WD Jr, Brenz R, McGrath CM, Russo J, Pauley RJ, Jones RF, Brooks SC. 1990. Isolation and

characterization of a spontaneously immortalized human breast epithelial cell line, MCF-10. Cancer Res. 50:6075–6086.

Summerer I, Unger K, Braselmann H, Schuettrumpf L, Maihoefer C, Baumeister P, Kirchner T, Niyazi M, Sage E, Specht HM, et al. 2015. Circulating microRNAs as prognostic therapy biomarkers in head and neck cancer patients. Br J Cancer. 113:76–82.

Tinoco G, Warsch S, Gluck S, Avancha K, Montero AJ. 2013. Treating breast cancer in the 21st century: emerging biological therapies. J Cancer. 4:117–132.

Wang P, Zou F, Zhang X, Li H, Dulak A, Tomko RJ Jr, Lazo JS, Wang Z, Zhang L, Yu J. 2009. microRNA-21 negatively regulates Cdc25A and cell cycle progression in colon cancer cells. Cancer Res. 69:8157–8165.

Yan LX, Wu QN, Zhang Y, Li YY, Liao DZ, Hou JH, Fu J, Zeng MS, Yun JP, Wu QL, et al. 2011. Knockdown of miR-21 in human breast cancer cell lines inhibits proliferation, *in vitro* migration and *in vivo* tumor growth. Breast Cancer Res. 13:R2.

Yang CH, Yue J, Pfeffer SR, Fan M, Paulus E, Hosni-Ahmed A, Sims M, Qayyum S, Davidoff AM, Handorf CR, et al. 2014. MicroRNA-21 promotes glioblastoma tumorigenesis by down-regulating insulin-like growth factor-binding protein-3 (IGFBP3). J Biol Chem. 289: 25079–25087.

Zhang ZJ, Ma SL. 2012. miRNAs in breast cancer tumorigenesis (Review). Oncol Rep. 27:903–910.